WILEY | Hindawi

Research Article

Pyrolysis Characteristics and Effect on Pore Structure of Jimsar Oil Shale Based on TG-FTIR-MS Analysis

Zhijun Liu [ID],[1,2] Haotian Ma,[1] Jianping Guo,[3] Gang Liu [ID],[1,2] Zhen Wang,[1] and Yuzhen Guo[1]

[1]College of Mining Engineering, Heilongjiang University of Science and Technology, Harbin 150022, China
[2]Heilongjiang Ground Pressure and Gas Control in Deep Mining Key Laboratory, Heilongjiang University of Science and Technology, Harbin 150022, China
[3]Xilingol League Qiantu Traffic Design Co., Ltd, Xilinhot 026000, China

Correspondence should be addressed to Zhijun Liu; 2004800167@usth.edu.cn

The study of the pyrolysis characteristics of oil shale, an important strategic resource, is of great significance for oil shale refining and in situ underground mining. In this study, using the oil shale from Jimsar region of Xinjiang, in combination with thermogravimetric analyzer (TG), Fourier transform infrared spectroscopy (FTIR), and mass spectrometry (MS) techniques, the pyrolysis characteristics and mechanism of the oil shale are analyzed according to the experimental results and explored the effect of its pyrolysis on the development of the pore. The results, the pyrolysis with three stages, show the following: (1) The first stage is 23-390°C. The precipitation of adsorbed water within the oil shale and the dehydration of gypsum are mainly at 100°C or so, appearing some microcapillary pores and other temperature sections change little. (2) The second stage is 390-527°C. The organic matter pyrolysis of Jimsar oil shale accounts for 71.1% of the total weight loss of oil shale. This stage has the greatest impact on the evolution of pore structure, and there are two weight loss peaks at 458°C and 506°C, respectively, in the thermogravimetric curve. Combined with FTIR-MS, the main products of its pyrolysis gas are H_2, H_2O, CO_2, CH_4, and C_nH_m and will change the original pore surface of oil shale, create new pore volume, and produce complex and irregular pore structure. (3) In third stage (527-800°C), the formation of H_2, CO_2, and hydrocarbon gases suggests that this stage includes not only the decomposition of major inorganic components like carbonate and clay but also the degradation process of some organic matter. At this stage, the CO_2 generated in the precipitation process will lead to a large number of pores in oil shale. Crack grids will appear, due to the melting and recrystallization of some clay minerals. Once the interaction between the two is particularly intense, the mineral skeleton may rupture and collapse. The pyrolysis characteristics above provide a basis for the analysis of the pore structure evolution of oil shale and are of implications and practical application value to the exploitation of shale oil.

1. Introduction

2021 is the key year of energy transformation, and the energy industry is facing severe challenges. According to the World Energy Council (WEC) [1], after the largest absolute decline of 4.5% in 2020, energy demand rebounded in 2021 as a result of the gradual lifting of new corona restrictions and economic recovery. The oil and gas industry is possible to enter a recovery phase by 2021, with international oil prices expected to rise year on year, according to the China Petroleum Daily [2]. By 2020, the crude oil dependence of China on foreign countries has reached 69%, which indicates that China has been highly unable to be self-sufficient in energy. As unconventional energy, the world's oil shale reserves contain approximately 6050 billion barrels of shale oil, which is four times that of conventional crude oil [3]. China's oil shale reserves are about 330 billion barrels, ranking second in the world. Therefore, its rich resources and comprehensive utilization value are more prominent [4].

The traditional exploitation and utilization of oil shale is ground distillation that has problems of cost, pollution, and

energy consumption and is out of step with the current trend of low-carbon and environmentally friendly development. Therefore, in situ mining of oil shale has emerged as a new trend in the development of mining technology, due to its advantages of large recoverable depth, high oil recovery rate, small footprint, and environmental protection. And oil shale, an organic-rich and fine-grained sedimentary rock, consists of a mineral porous matrix that contains insoluble kerogen, quartz, clay minerals, and other substances. With the increase in temperature, the organic matter and inorganic minerals in oil shale will undergo complex physical and chemical reactions, which will have a direct impact on the evolution of the pore structure of oil shale, thus affecting the exploitation of shale oil. In this process, the internal organic matter is pyrolyzed, and some inorganic minerals are decomposed, and the internal structure will inevitably change, thus affecting the evolution of pores. At the same time, the thermal expansion force inside the oil shale also affects the evolution of its pore structure, so it is feasible to study the pore evolution law through the material composition of the oil shale.

At present, research has made great progress in the pyrolysis characteristics of oil shale, and different scholars have analyzed the pyrolysis mechanism from multiple perspectives. Campbell et al. [5] conducted nonisothermal rate pyrolysis kinetics analysis on pyrolysis gas of Colorado oil shale and considered that the pyrolysis of kerogen could be divided into carbonaceous residue and liquid, gaseous, and hydrocarbons; carbonaceous residue and gaseous; and carbonaceous residue and gas three stages. Williams and Chishti [6] investigated the effect of pyrolysis reaction residence time on oil shale pyrolysis. Yue et al. [7] concluded that increasing pyrolysis temperature has a greater impact on the yield of oil shale pyrolysis products than residence time. Based on the influence of heating rate on the decomposition of organic matter in oil shale, using TG and MS techniques to the pyrolysis of Green River oil shale at different heating rates, Tiwari and Deo [8] show that the ratio of olefins to alkanes increased with the increase of heating rate. Wang et al. [9] established the three-dimensional model of kerogen by simulating annealing dynamics and performing geometric optimization. Through the infrared experiment of minerals, Lan et al. [10] found that the maximum weight loss temperature of oil shale was higher than that of kerogen, and the activation energy was calculated by the model. Han et al. [11] found through experiments that shale oil production increased significantly with the increase of distillation temperature and recommended the distillation temperature of 460–490°C. Due to the adsorption of clay minerals on native asphalt in organic matter, Borrego et al. [12] show that the initial weight loss temperature of oil shale pyrolysis is significantly higher than that of organic matter pyrolysis alone. Karabakan and Yürüm [13] thought that alkaline metal cations in carbonate catalyzed the pyrolysis reaction, while silicate inhibited the pyrolysis reaction, and the inhibition of silicate was greater than that of carbonate. Meantime, some scholars, based on the combination of CT technology and three-dimensional reconstruction, studied the structure of pores during oil shale pyrolysis. On the pyrolysis of oil

shale research, Zhao et al. [14] found that different mineral compositions under the action of temperature have different physical and chemical reactions that lead to oil shale rupture. Additionally, mineral particles and matrix cementation way and degree affect the difficulty of oil shale rupture. Zhang et al. [15] found that oil shale after bioleaching will produce a large number of micropores, which is conducive to transferring heat from the outside to the inside of the oil shale sample and helping to produce more shale oil. Wang et al. [16] considered that the pore connectivity caused by the generation and migration in pyrolysis products was an important factor for the increase of porosity. Through the study of Fushun oil shale, Geng et al. [17] found that with the increase in temperature, the length and opening of cracks became larger, the porosity and the degree of pyrolysis increased gradually, and the number of cracks and the maximum porosity increased gradually. Eseme et al. [18] found that during the pyrolysis process, the microscopic pore structure and physicochemical properties of oil shale interacted and changed significantly. Yang et al. [19] found that the total pore volume, average pore diameter, and porosity of oil shale increased significantly with the increase in temperature. In the heating process of oil shale, the volume of mesopores increases, and the volume of micropores decreases continuously.

In summary, presently there are fruitful results in the study of pore structure and material composition, but there are few studies to explain the evolution law of pore structure through the basic material composition and the reaction of oil shale. Therefore, the purpose of this study is to research the changes in mineral composition and product formation in the pyrolysis process of Jimsar oil shale; what is more, discuss the influence of pyrolysis on pore development by combining the TG, FTIR, and MS techniques. This research, on a theoretical basis, is crucial to the technology for in situ oil shale extraction.

2. Materials and Methods

2.1. Preparation of Oil Shale Samples. Oil shale samples were collected from the Shichanggou Mine of Jimsar County in the Xinjiang Province, China, which belongs to the Permian Lucaogou Formation. With the simple structure, it is mainly composed of lagoon facies. The thickness of the ore body is 18.80–63.20 m, and the ore body mainly composed of striation and phyllotactic structure, grayish black or gray, and locally lenticular. The oil shale samples were sealed immediately using paraffin wax to avoid weathering and deterioration. After that, they were broken to particle sizes less than 75 μm [11, 20] and dried for 12 h at 70°C for use in pyrolysis experiments.

The element analysis and industrial analysis of samples of initial oil shale were determined according to the national standards GB/T 212-2008 and GB476-91, respectively (Table 1). The mineral composition of the sample was determined by using a Rigaku D/Max-2500 X-ray diffractometer (manufactured by Shimadzu, Kyoto, Japan) (Table 2). XRD data was recorded at 45 kV and 100 mA, at a scan rate of 2°/min (whole rock), scanning range 2.6–45° (whole rock

TABLE 1: Element analysis and industrial analysis of oil shale.

Elementary analysis						Industrial analysis			
N%	C%	H%	O%	H/C	O/C	Moisture	Ash	Volatile	Fixed carbon
1.36	9.27	1.98	8.865	2.56	0.72	5.44	82.25	10.32	1.99

TABLE 2: Mineral composition of oil shales.

Mineral composition (%)							
Quartz	Pyrite	Clay	Sanidine	Plagioclase	Calcite	Dolomite	Gypsum
36.1	0.6	5	8.2	26.8	3.6	19	0.7

analysis). According to Table 2, the quartz, plagioclase, and dolomite are the primary mineral components of the oil shale, followed by sanidine, calcite, and clay minerals and smaller amounts of pyrite and gypsum.

2.2. TG-FTIR-MS Experiment. TG-FTIR-MS was used to analyze the pyrolysis process of oil shale and pyrolysis gas products, as shown in Figure 1. The system is composed of a SETSYS Evolution 16/18 synchronous thermal analyzer (Setaram Co, Caluire, France), a TENSOR27 infrared spectrophotometer (Bruker, Germany), and an OMNI star mass spectrometer (Pfeiffer, Germany). The instruments were connected by heating quartz capillary to prevent the error of experimental results caused by condensation of vapor and other gas components in the experiment. The TG resolution of this equipment is $0.03\,\mu$g, and the vacuum degree is 10^{-4} mbar. The FTIR resolution is $4\,cm^{-1}$, the scanning times is 4, the spectral range is $8000\text{-}350\,cm^{-1}$, and the wavenumber accuracy is $0.01\,cm^{-1}$. The MS detection range is 1-300 amu in high vacuum conditions, and the capillary operating temperature is $200°C$.

In this study, about 20 mg of oil shale samples were evenly distributed at the bottom of the thermogravimetry crucible and heated to $800°C$ at a rate of $10°C/min$ [21] using nitrogen as a protective gas. In the thermal separation process of the TG analyzer, the gas produced by the pyrolysis of the sample in TG was transported to the FTIR and MS in real-time through nitrogen purge, and infrared data acquisition and mass spectrometry detection were carried out, respectively.

3. Results

3.1. Experimental Results and Analysis Based on TG. During the heating process of Jimsar oil shale, with the increase of temperature, the oil shale undergoes physical and chemical changes such as decomposition and dehydration. The TG/DTG curves of pyrolysis of oil shale are shown in Figure 2. The TG/DTG curves are consistent with the weight loss trend of reference [22] and described the weight loss and weight loss rate of samples with the increase of temperature, respectively.

According to Figure 2, The total weight loss of the oil shale was 20.4%. The pyrolysis process can be divided into three stages. In the first stage, between 23 and $390°C$, the first

main weight loss stage of Jimsar oil shale appears at about $100°C$. There were two peak weight losses corresponding to 73 and $100°C$ in the DTG curve, and the weight loss was 0.3%. According to Table 2, it is speculated that the two weight loss peaks on the DTG curve should correspond to two asynchronous but overlapping reactions of the precipitation of adsorbed water and gypsum dehydration, respectively, due to the dehydration reaction of gypsum in Jimsar oil shale at $100°C$ [23]. The second stage, between 390 and $527°C$, is the main oil shale pyrolysis stage; weight loss in this stage was 14.5%. It accounted for 71.1% of the total weight loss and had the greatest impact on the composition of substances. There are two obvious weight loss peaks in the DTG curve, which can be divided into two substages. Stage I ranges from 390 to $488°C$. The weight loss peak is located at $458°C$, and the weight loss is about 12.2%. This is owing to the intense chemical reaction of organic matter in oil shale, and a large amount of pyrolysis gas is precipitated from the pyrolysis of oil shale, and more aliphatic and aromatic compounds are produced [22, 24, 25]. Phase II ranges from 488 to $527°C$. The weight loss peak is located at $506°C$, and the weight loss is about 2.3%. This peak indicates that new chemical reactions occur in oil shale around $506°C$, which is analyzed as the secondary reaction of pyrolysis products, petroliferous cracking [26], in phase I, and is the thermal decomposition of hydrocarbon compounds with a large mass. And the unstable intermediate produced in stage I is high maturity bitumen, which is conducive to connecting open and closed pores and promoting oil and gas transportation. The third stage, $527\text{-}800°C$, had a weight loss of 2.9%, and the peak of weight loss is located at $658°C$. Weight loss in the third stage is related to the decomposition of inorganic matter, especially the decomposition of carbonate minerals such as dolomite and may be related to the cracking and degradation of polycyclic aromatic hydrocarbons. And there is also a weight loss peak at about $790°C$, which is due to the thermal decomposition of calcite in Jimsar oil shale, and this part is slightly different from the pyrolysis process of Fushun oil shale [27], indicating that the composition of oil shale in different regions is different, resulting in some differences in its pyrolysis characteristics.

In summary, during the whole pyrolysis process of oil shale, the first stage is the desorption of internal free water, adsorbed water, and adsorbed gas in oil shale samples. The second stage is kerogen decomposition in oil shale,
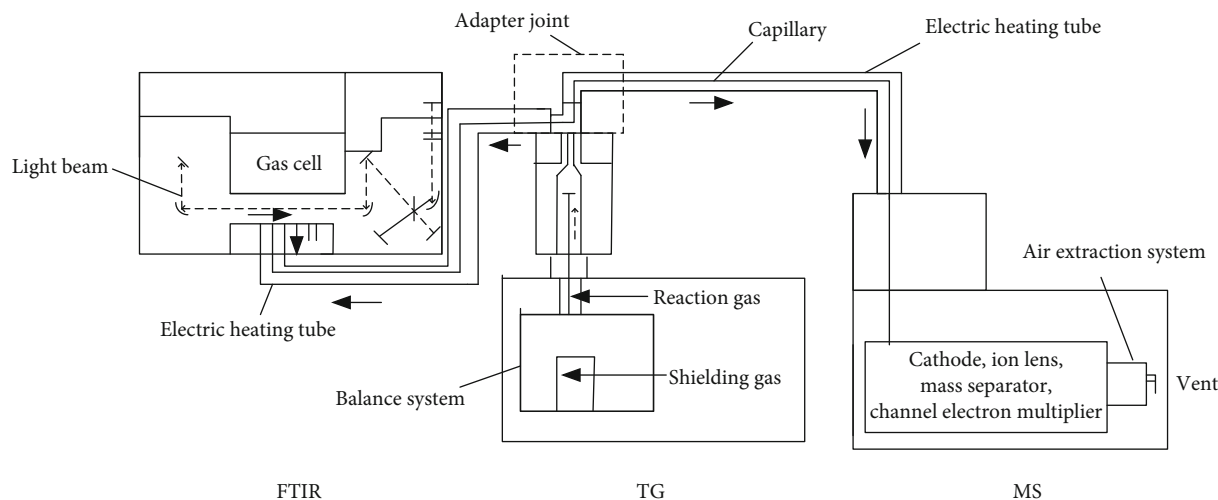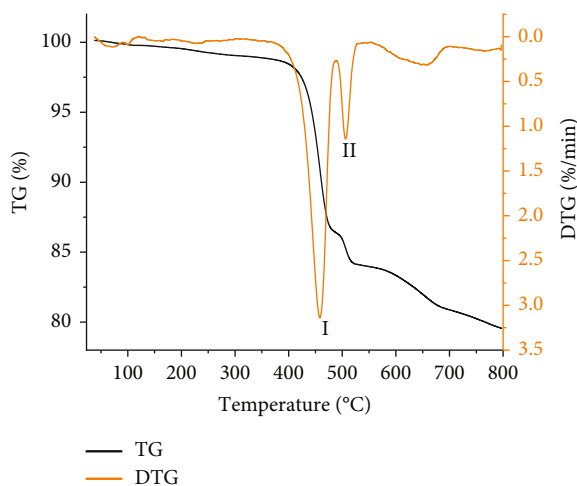
FɪɢᴜRᴇ 1: Experimental principle of TG-FTIR-MS.

FɪɢᴜRᴇ 2: TG/DTG curve of Xinjiang oil shale.

producing unstable intermediate and gaseous products; with the gradual increase of heating temperature, unstable intermediates produce secondary cracking and release some gaseous products to form more stable intermediates. The third stage is the phase transformation decomposition of some inorganic components such as carbonates and clay minerals in oil shale at higher temperatures. The starting and ending temperatures of this stage are mainly related to the composition of inorganic substances. At the same time, Jimsar oil shale still has gaseous products at this stage due to its high degree of metamorphism.

3.2. Experimental Results and Analysis Based on MS. In general, the chemical reaction process of oil shale pyrolysis is the branch chain fracture of kerogen, the rupture of ether bond or carbon-carbon single bond between benzene rings, and the ring cracking and degradation of thick rings. With the pyrolysis of functional groups, the macromolecular of oil shale is degraded into small molecules with low boiling point and precipitated in the form of gas at the reaction tem-

perature. These gaseous compounds can be detected by the MS technique. The following is to characterize the gas precipitation law under the action of temperature by the ion current intensity of gas fragments with a fixed mass-to-charge ratio at different temperatures. The change law of ion current intensity reflects the precipitation concentration of corresponding gas and ion fragments. Figures 3(a)–3(e) are mass spectrum curves of major light gases H_2 ($m/z = 2$), H_2O ($m/z = 18$), CH_4 ($m/z = 15$, 16), and CO_2 ($m/z = 44$) and light hydrocarbons C_nH_m (hydrocarbons and fragments with C atom number less than 4 outside CH_4) during pyrolysis of Jimsar oil shale.

According to Figure 3(a), the precipitation of H_2 is obviously divided into two stages. The first stage occurs in the temperature range of 400–545°C, and there are two intensity peaks at 477 and 515°C, respectively. The second stage is from 545 to 800°C, and the ion current intensity of H_2 continues to increase. At this stage, H_2 comes from the decomposition of condensed aromatic and aromatic structures or heterocyclic compounds [28, 29]. The temperature of H_2 production is consistent with TG weight loss temperature, which further shows that the pyrolysis and condensation between small molecules first occur in the oil shale, releasing H_2. With the increase of temperature, sphere-like molecule further reacts to release H_2 or through $H_2O + CO_2$——$CO + H_2$ reaction to release H_2. As shown in Figure 3(b), the precipitation characteristics of H_2O in the oil shale show an obvious stage. Jimsar oil shale in the first stage of precipitation water is more obvious, mainly from the precipitation of adsorbed water and gypsum dehydration in the sample; the second precipitation peak appeared in the range of 410–500°C, and the peak intensity was less. The CH_4 curve of the Jimsar oil shale is shown in Figure 3(c), and there are two stages of CH_4 precipitation in the curve. The first stage occurs in the temperature range of 400–573°C, and there are two peaks at 480°C and 515°C, respectively. In the second stage, the precipitation occurs in the temperature range of 570–710°C, and the peak point corresponds to the temperature of 671°C. In this stage, CH_4 comes from the
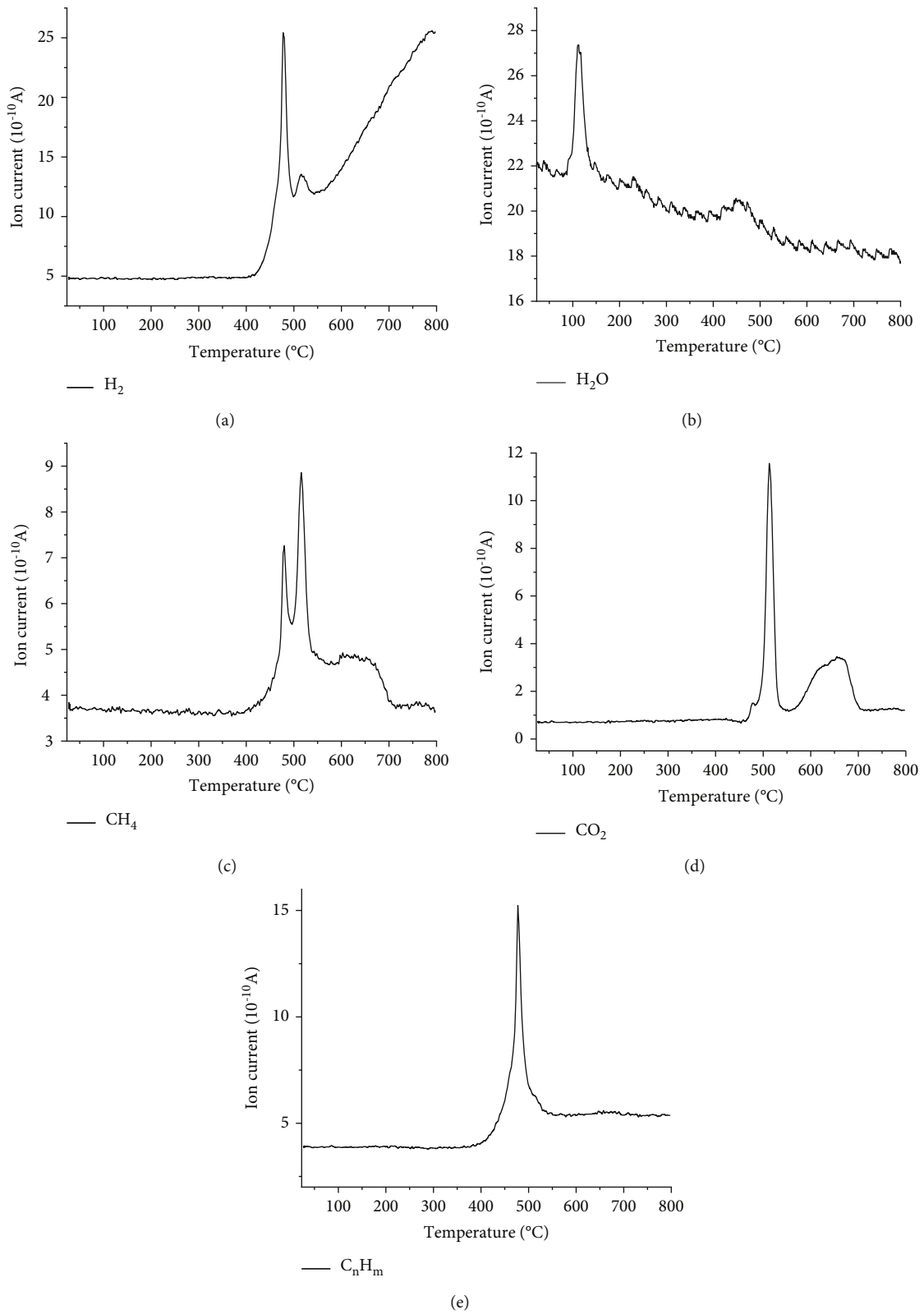
(a)

(b)

(c)

(d)

(e)

FIGURE 3: Mass spectrogram of oil shale. (a) H_2, (b) H_2O, (c) CH_4, (d) CO_2, and (e) C_nH_m.

bond fracture between aromatic methyl or aromatic alkyl [8, 30] This corresponds to two peaks in the third stage of the DTG curve. The reason for this result is that the organic matter composition and structure of Jimsar oil shale are

complex, and the pyrolysis process needs to be decomposed step by step at different temperatures. According to Figure 3(d), the thermal desorption process of CO_2 from Jimsar oil shale shows two stages. The first stage is located

in the temperature range of 454–550°C. In the interval, there is an obvious indigenous strength peak at 513°C, and there is a weak strength peak at 477°C. The strength peak near 477°C is caused by the decomposition of aliphatic and aromatic carboxyl groups in oil shale. With the increase of temperature, ether structure and oxygen-containing carbonyl functional groups in oil shale are broken. In addition to some escaping in the form of CO, some combine with oxygen atoms to form CO_2, thus generating the second precipitation peak at 513°C. The second stage occurs in the range of 550–715°C, and the peak width is large, which is mainly generated by the decomposition of minerals such as carbonate. Hydrocarbons are the main products of oil shale pyrolysis. The law of hydrocarbon substances (C_nH_m) from oil shale pyrolysis is shown in Figure 3(e). Hydrocarbon organic matter in the whole pyrolysis process only in 400-542°C interval appeared an obvious strength peak; the width is small, and the peak is at 477°C (corresponding to the first peak of CH_4 precipitation). After 542°C, the ion current intensity was significantly higher than that before the peak, indicating that a small amount of C_nH_m light gas continued to precipitate.

Summary of the above MS analysis found that after 550°C, whether CH_4 or C_nH_m showed a sustained and slow release trend, indicating that under the temperature conditions, Jimsar oil shale organic matter in the continuous cracking. The above MS analysis has high consistency with the weight loss law and mineral composition in a TG analysis of oil shale.

3.3. Experimental Results and Analysis Based on FTIR.

According to the FTIR absorption spectra of different gas products, combined with the infrared analysis of oil shale gas products and peak separation technology [9, 31, 32], the characteristic absorption peaks of some gases and functional groups in gas products are determined as listed in Table 3.

The FTIR spectra of pyrolysis gas products are shown in Figure 4. Combined with Figure 4 and Table 3, it can be seen that the pyrolysis products of Jimsar oil shale mainly contain CH_4, CO_2, H_2O, and C_nH_m. In the range of 23–400°C, only CO_2 and H_2O were detected in the infrared gas; at 450°C, there were relatively obvious C_nH_m peaks at $2929\,cm^{-1}$ and $2858\,cm^{-1}$, respectively, and a large number of aliphatic hydrocarbon gases were precipitated. At 500°C, the C_nH_m intensity peak decreased significantly, while the H_2O and CO_2 intensity peaks reached the maximum value in the whole pyrolysis range, reflecting the obvious staged pyrolysis characteristics of Jimsar oil shale, and each peak decreased at 550°C. The intensity peaks of H_2O and CO_2 at 600°C reached the second peak in the heating range, mainly for the decomposition of carbonate minerals such as dolomite and calcite in oil shale to produce gas; the infrared spectra after 600°C was mainly characterized by H_2O and CO_2, which was consistent with MS and TG/DTG analysis.

The precipitation of H_2O and CO_2 in the pyrolysis process of organic matter lags behind that of hydrocarbon gases, which is due to the direct correlation between the pyrolysis process of oil shale and the structure of kerogen. The kero-

gen is composed of polycyclic aromatic hydrocarbons with different aromatization degrees and is connected by bridge bonds such as carbon and ether oxygen, and there are a large number of branched structures. Due to the different compositions of polycyclic aromatic hydrocarbons, the bond energies are different, and the pyrolysis temperatures are inconsistent. The more stable the structure is, the more activation energy is needed and the higher the cracking temperature is. In addition, as a homonuclear diatomic molecule, the dipole moment does not change during vibration and rotation, which is always 0, so there is no absorption peak of H_2 in the infrared [33], but this does not mean that there is no H_2 precipitation in the product. Additionally, after 500°C the peak at $3255\,cm^{-1}$ of Jimsar oil shale was found to have a low strength and peak width; the reason may be due to the stretching vibration of O-H bond in the association of alcohols and phenols. In the experiment, when the organic matter of oil shale reaches the pyrolysis temperature, a large number of compounds undergo complex chemical reactions in a short period time, and some products have similar FTIR spectra. Therefore, in addition to the above gases with obvious aboriginal absorption peaks, the characteristic spectra of more complex organic compounds in gas products are not obvious.

4. Discussion

In these experiments, the pyrolysis of oil shale includes three stages. In these stages, with the increase of temperature, a series of physical and chemical reactions occur in the internal material of oil shale, and the material composition changes, which will inevitably lead to changes in the pore structure of oil shale.

In the first stage, due to the dehydration of adsorbed water and gypsum in the oil shale, there is no significant change in the overall oil shale at this time. When the crystal water of gypsum is removed, the volume of gypsum in the oil shale decreases, resulting in microcapillary pores. This is consistent with the conclusion of Saif et al. [34] that the porosity of $2\,\mu m$ voxel size does not change significantly between 20°C and 380°C. And Jin et al. [35] and Meng et al. [36] found that at low temperature (23-390°C), the main reason of oil shale fracture is caused by thermal stress and mineral water loss and thermal expansion without binding state produced more pores. Combined with the pyrolysis experiment at 100–390°C, there is no obvious weight loss phenomenon in oil shale. It is indicated that at this time, the internal oil shale is mainly due to the different thermal expansion coefficients of each component. The expansion force of each component may lead to the expansion of the original fracture and generate more pores.

In the second stage (390–527°C), the oil shale of Jimsar is the main weight loss stage. In the in situ mining of oil shale, shale oil and gas produced by oil shale pyrolysis will be transported to the ground with the pores and cracks inside oil shale. In this process, with the increase of temperature, the softening or carbonization of organic matter in oil shale will affect the pore structure parameters [37]. When the organic matter is pyrolyzed, the high-maturity bitumen

TABLE 3: Main absorption peaks of FTIR spectra of gas products from pyrolysis of oil shale.

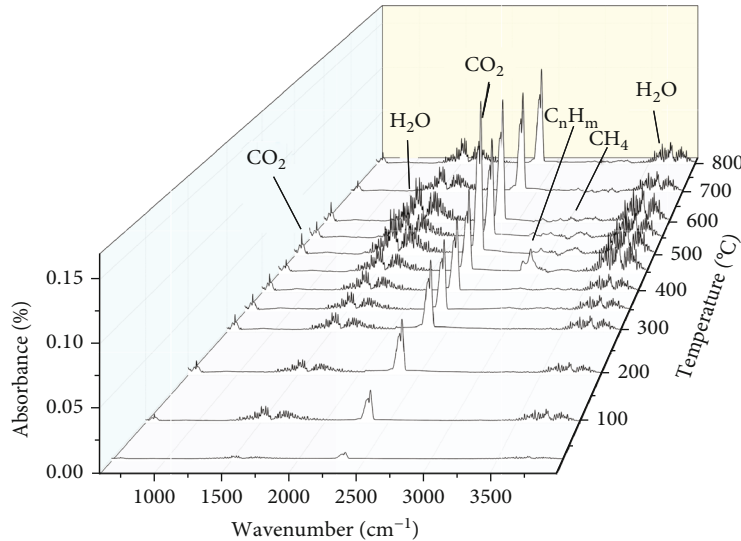| Gaseous product	Peak range (cm^{-1})	Absorption peak-position (cm^{-1})	Functional group	Vibrational modes
CH_4	3000 - 3024	3012	C-H	Stretching vibrations
CO_2	600-725 2240 - 2400	669 2360	C=O	Stretching vibrations
H_2O	4000-3500 1900 - 1300	3638, 3735 1508	O-H	Stretching vibrations
C_nH_m	3000 - 2800	2929, 2858	C-H	Stretching vibrations

FIGURE 4: IR spectra of gas products in the process of Xinjiang oil shale pyrolysis.

generated in stage I will block the pores and reduce the pore surface area [38, 39] Entering stage II, the high-maturity bitumen reacts twice to produce shale oil, which at the same time leads to a strong fracture with the original bedding structure of shale, leading to the expansion of pores and higher pore connectivity [40]. And the violent release of volatile substances will change the original pore surface of oil shale, creating new pore volume and produce complex and irregular pore structure. This is associated with Bai et al. [41] who found that a large number of shale oil vapor and fuel gas erupted rapidly, which will lead to the opening of pores, and the increase in the number of micro, medium, and large pores and the oil shale samples can clearly see cracks and fractures by scanning electron microscopy at 400°C. This is consistent with Liu et al. [27] who found that the thermal response mechanism of organic matter and minerals in oil shale at each temperature stage is different and affects the change of pore structure—at 350°C, the pore shape changed significantly and began to thermal decomposition. The pore volume, porosity, and specific surface area (SSA) of oil shale samples increased rapidly with the change of temperature from 350 to 600°C. It was also consistent with the average porosity of the sample at 400°C as mentioned by Saif [42], which was 8.6%. As the temperature increased to 500°C, the average porosity of the sample also increased to 21.9%. Therefore, at this stage, with the sub-

stantial increase of pores, the production of oil and gas gradually increases to the maximum.

In the third stage, the mineral composition in oil shale changes. With the increase of temperature, the constraints caused by different expansion rates of each component increase. When the thermal stress reaches the yield strength of oil shale material, more new cracks are formed and extended along the boundaries of different grains. The width and length of cracks increase significantly, and a certain number of secondary cracks are generated at the edge of the main crack. In addition, the temperature has a damage effect on the crystal structure of quartz, and the α and β phase transformation of quartz in oil shale is also conducive to fracture propagation [41]. When the temperature is above 600°C, the decomposition of carbonate minerals such as dolomite will produce a large amount of CO_2, and the CO_2 in the precipitation process will lead to a large number of pores in oil shale. At the same time, due to the melting and recrystallization of some clay minerals, there will be cracks in the grid, which will even lead to the fracture and collapse of the mineral skeleton.

5. Conclusions

Based on the mineral composition and TG-FTIR-MS analysis of the Jimsar oil shale, the variation law of oil shale with

temperature as well as the pyrolysis characteristics and product formation law of oil shale was found. And then discuss the pyrolysis mechanism. Conclusions are as follows:

(1) According to the TG experiment, the mass loss and loss rate of the experimental samples with the increase in temperature were analyzed. The results show that the TG/DTG curves of oil shale shows three stages of weight loss: free water precipitation stage, organic matter pyrolysis stage, and inorganic mineral decomposition stage. The organic matter pyrolysis stage is the main weight loss stage of oil shale, and there are two weight loss peaks in the DTG curve of Jimsar oil shale. In addition, organic matter in Jimsar oil shale is still cracking in the third stage

(2) Based on the MS and FTIR analysis of pyrolysis gas products, it is determined that the pyrolysis gas products of oil shale mainly include H_2, H_2O, CH_4, CO_2, and C_nH_m. The products in each stage and their relationship with temperature are closely related to the kerogen metamorphic degree and inorganic mineral composition of oil shale. The precipitation of H_2, CH_4, and CnHm is mainly caused by the pyrolysis of organic matter, and the production of H_2O and CO_2 is related to the pyrolysis of organic matter and the decomposition of carbonate minerals. Besides, the precipitation of H_2O in the low-temperature section is also related to mineral water absorption. In addition, it was found that the TG reaction in the third stage of Jimsar oil shale contained the degradation reaction of organic matter, indicating that oil shale had a high degree of metamorphism, and thermal cracking of some fused ring contained in it required higher temperature

(3) With the temperature increased, the pore structure parameters of Jimsar oil shale changed. Before 390°C, the pore water in oil shale is mainly removed. The inorganic minerals are slightly adjusted under the action of thermal stress, and the pore structure parameters change little. The temperature range, 390–527°C, is significantly affected by the pyrolysis of organic matter, the pore pressure formed by oil and gas products, and the thermal cracking of inorganic minerals. The pore volume changes in the 527-800°C temperature range due to the decomposition of carbonate minerals, SiO_2 phase transition, and a small part of polycyclic aromatic hydrocarbons cracking, as well as the fracture and collapse of a mineral skeleton

Data Availability

The data used to support the findings of this study have not been made available because the original data relate to the intellectual property rights of the author, and all the original data cannot appear in the paper, and the experimental data that cannot appear is related to privacy.

References

[1] World Energy Council, "World Energy Issues Monitor 2022," 2022, https://www.worldenergy.org/publications/entry/world-energy-issues-monitor-2022/.

[2] X. Y. Wang, "Oil markets show prospects for recovery but remain cautious," *China Petroleum Daily*, vol. 9, article 8, 2021.

[3] J. R. Dyni, "Geology and resources of some world oil-shale deposits," *Oil Shale*, vol. 20, pp. 193–252, 2003.

[4] S. H. Mohr, J. Wang, G. Ellem, J. Ward, and D. Giurco, "Projection of world fossil fuels by country," *Fuel*, vol. 141, pp. 120–135, 2015.

[5] J. H. Campbell, G. Gallegos, and M. Gregg, "Gas evolution during oil shale pyrolysis. 2. Kinetic and stoichiometric analysis," *Fuel*, vol. 59, no. 10, pp. 727–732, 1980.

[6] P. T. Williams and H. M. Chishti, "Influence of residence time and catalyst regeneration on the pyrolysis-zeolite catalysis of oil shale," *Journal of Analytical and Applied Pyrolysis*, vol. 60, no. 2, pp. 187–203, 2001.

[7] C. Yue, Y. Liu, Y. Ma, S. Li, J. He, and D. Qiu, "Influence of retorting conditions on the pyrolysis of Yaojie oil shale," *Oil Shale*, vol. 31, no. 1, pp. 66–78, 2014.

[8] P. Tiwari and M. Deo, "Compositional and kinetic analysis of oil shale pyrolysis using TGA-MS," *Fuel*, vol. 94, pp. 333–341, 2012.

[9] Q. Wang, Z. Y. Xie, C. X. Jia, and C. A. Li, "Characteristics of gases evolution during Huadian oil shale pyrolysis," *Chemical Industry and Engineering Progress*, vol. 36, pp. 4416–4422, 2017.

[10] X. Z. Lan, W. J. Luo, Y. H. Song, J. Zhou, and Q. L. Zhang, "Effect of the temperature on the characteristics of retorting products obtained by Yaojie oil shale pyrolysis," *Energy & Fuels*, vol. 29, no. 12, pp. 7800–7806, 2015.

[11] X. X. Han, X. M. Jiang, and Z. G. Cui, "Studies of the effect of retorting factors on the yield of shale oil for a new comprehensive utilization technology of oil shale," *Applied Energy*, vol. 86, no. 11, pp. 2381–2385, 2009.

[12] A. G. Borrego, J. G. Prado, E. Fuente, M. D. Guillén, and C. G. Blanco, "Pyrolytic behavior of Spanish oil shales and their kerogens," *Journal of Analytical & Applied Pyrolysis*, vol. 56, no. 1, pp. 1–21, 2000.

[13] A. Karabakan and Y. Yürüm, "Effect of the mineral matrix in the reactions of oil shales: 1. Pyrolysis reactions of Turkish Goynuk and US Green River oil shales," *Fuel*, vol. 77, no. 12, pp. 1303–1309, 1998.

[14] J. Zhao, D. Yang, Z. Q. Kang, and Z. C. Feng, "A micro-CT study of changes in the internal structure of Daqing and Yan'an oil shales at high temperatures," *Oil Shale*, vol. 29, no. 4, pp. 357–367, 2012.

[15] X. Q. Zhang, Y. H. Fei, Y. S. Li, B. Zhou, H. J. Ren, and L. Y. Zhang, "Effect of bioleaching on the yield and composition of Meihekou oil shale (China)," *Oil Shale*, vol. 31, no. 2, pp. 174–184, 2014.

[16] Q. Wang, G. J. Jiao, H. P. Liu, J. R. Bai, and S. H. Li, "Variation of the pore structure during microwave pyrolysis of oil shale," *Oil Shale*, vol. 27, no. 2, pp. 135–146, 2010.

[17] Y. D. Geng, W. G. Liang, J. Liu, M. T. Cai, and Z. Q. Kang, "Evolution of pore and fracture structure of oil shale under high temperature and high pressure," *Energy & Fuels*, vol. 31, no. 10, pp. 10404–10413, 2017.

[18] E. Eseme, J. L. Urai, B. M. Krooss, and R. Littke, "Review of mechanical properties of oil shales: implications for exploitation and basin modelling," *Oil Shale*, vol. 24, no. 2, pp. 159–174, 2007.

[19] L. S. Yang, D. Yang, J. Zhao, Z. H. Liu, and Z. Q. Kang, "Changes of oil shale pore structure and permeability at different temperatures," *Oil Shale*, vol. 33, no. 2, pp. 101–110, 2016.

[20] H. L. Yu and X. M. Jiang, "Influence of Particle Diameter on Pyrolysis Property and Kinetic Parameter of Oil Shale," *Journal of Zhongyuan Institute of Technology*, vol. 18, pp. 1–4, 2007.

[21] T. Kaljuvee, J. Pelt, and M. Radin, "TG-FTIR study of gaseous compounds evolved at thermooxidation of oil shale," *Thermal Analysis and Calorimetry*, vol. 78, no. 2, pp. 399–414, 2004.

[22] L. W. Pan, F. Q. Dai, G. Q. Li, and S. Liu, "A TGA/DTA-MS investigation to the influence of process conditions on the pyrolysis of Jimsar oil shale," *Energy*, vol. 86, pp. 749–757, 2015.

[23] C. A. Strydom, D. L. Hudson-Lamb, J. H. Potgieter, and E. Dagg, "The thermal dehydration of synthetic gypsum," *Thermochimica Acta*, vol. 269, pp. 631–638, 1995.

[24] D. Skala, M. Bastić, J. Jovanović, and I. Rahimian, "Pyrolysis of oil shale in a microretorting unit," *Fuel*, vol. 72, no. 6, pp. 829–835, 1993.

[25] Q. Q. Liu, X. X. Han, Q. Y. Li, Y. R. Huang, and X. M. Jiang, "TG–DSC analysis of pyrolysis process of two Chinese oil shales," *Journal of Thermal Analysis and Calorimetry*, vol. 116, no. 1, pp. 511–517, 2014.

[26] D. Lai, Y. Shi, S. Geng et al., "Secondary reactions in oil shale pyrolysis by solid heat carrier in a moving bed with internals," *Fuel*, vol. 173, pp. 138–145, 2016.

[27] Z. J. Liu, D. Yang, Y. Q. Hu et al., "Influence of in situ pyrolysis on the evolution of pore structure of oil shale," *Energies*, vol. 11, no. 4, article 755, 2018.

[28] X. Q. Li, B. M. Krooss, P. Weniger, and R. Littke, "Liberation of molecular hydrogen (H_2) and methane (CH_4) during non-isothermal pyrolysis of shales and coals: Systematics and quantification," *International Journal of Coal Geology*, vol. 137, pp. 152–164, 2015.

[29] P. T. Williams and N. Ahmad, "Influence of process conditions on the pyrolysis of Pakistani oil shales," *Fuel*, vol. 78, no. 6, pp. 653–662, 1999.

[30] A. Jess, "Mechanisms and kinetics of thermal reactions of aromatic hydrocarbons from pyrolysis of solid fuels," *Fuel*, vol. 75, no. 12, pp. 1441–1448, 1996.

[31] J. W. Yan, X. M. Jiang, X. X. Han, and J. G. Liu, "A TG-FTIR investigation to the catalytic effect of mineral matrix in oil shale on the pyrolysis and combustion of kerogen," *Fuel*, vol. 104, pp. 307–317, 2013.

[32] K. N. Alstadt, D. R. Katti, and K. S. Katti, "An _in situ_ FTIR step-scan photoacoustic investigation of kerogen and minerals in oil shale," *Spectrochimica Acta Part A: Molecular and Biomocular Spectroscopy*, vol. 89, pp. 105–113, 2012.

[33] J. Y. Nan, "The mechanism of infrared generation —— biatomic and molecular infrared spectroscopy," *Physics Bulletin*, vol. 5, pp. 11–13, 1996.

[34] T. Saif, Q. Y. Lin, K. Singh, B. Bijeljic, and M. J. Blunt, "Dynamic imaging of oil shale pyrolysis using synchrotron X-ray microtomography," *Geophysical Research Letters*, vol. 43, no. 13, pp. 6799–6807, 2016.

[35] P. H. Jin, Y. Q. Hu, J. X. Shao, Z. Liu, G. Feng, and S. Song, "Influence of temperature on the structure of pore–fracture of sandstone," *Rock Mechanics and Rock Engineering*, vol. 53, no. 1, pp. 1–12, 2020.

[36] Q. R. Meng, Z. Q. Kang, Y. S. Zhao, and D. Yang, "Experiment of thermal cracking and crack initiation mechanism of oil shale," *Journal of China University of Petroleum Natural Science*, vol. 34, pp. 89–92, 2010.

[37] X. X. Han, X. M. Jiang, Z. G. Cui, J. W. Yan, and J. G. Liu, "Effects of retorting factors on combustion properties of shale char. 2. Pore structure," *Energy & Fuels*, vol. 25, no. 1, pp. 97–102, 2011.

[38] L. N. Sun, J. C. Tuo, M. F. Zhang, C. Wu, Z. Wang, and Y. Zheng, "Formation and development of the pore structure in Chang 7 member oil-shale from Ordos Basin during organic matter evolution induced by hydrous pyrolysis," *Fuel*, vol. 158, pp. 549–557, 2015.

[39] J. T. Schrodt and A. Ocampo, "Variations in the pore structure of oil shales during retorting and combustion," *Fuel*, vol. 63, no. 11, pp. 1523–1527, 1984.

[40] L. Ribas, J. M. D. R. Neto, A. B. França, and H. K. P. Alegre, "The behavior of Irati oil shale before and after the pyrolysis process," *Journal of Petroleum Science and Engineering*, vol. 152, pp. 156–164, 2017.

[41] F. T. Bai, Y. H. Sun, Y. M. Liu, and M. Y. Guo, "Evaluation of the porous structure of Huadian oil shale during pyrolysis using multiple approaches," *Fuel*, vol. 187, pp. 1–8, 2017.

[42] T. Saif, Q. Y. Lin, B. Bijeljic, and M. J. Blunt, "Microstructural imaging and characterization of oil shale before and after pyrolysis," *Fuel*, vol. 197, pp. 562–574, 2017.